

BURST ACTIVITY AND HEART RHYTHM MODULATION IN THE SYMPATHETIC OUTFLOW TO THE HEART

G. Baselli¹, C. Falcomatà¹, F. Gelain¹, S. Cerutti¹, M. Massimini², N. Montano², A. Porta²

¹Department of Biomedical Engineering, Polytechnic University of Milan, Milan, Italy

²DiSP LITA "Vialba", "L.Sacco" Hospital, University of Milan, Milan, Italy

Abstract - In 13 decerebrate, artificially ventilated cats preganglionic sympathetic outflow to the heart was recorded with ECG and ventilation signal. A novel algorithm was implemented that extracts weighted events representing burst occurrences and their size. A multiple threshold strategy was used to separate bursts. Weighted events yielded count signals. Spectral analysis of the count signal revealed a predominance of a discharge synchronous to heart beat at cardiac frequency (CF@3 Hz), a ventilation rhythm at the high frequency (HF@0.3 Hz) of beat-to-beat variability, and in 9 of 13 cats a Mayer's wave lower frequency (LF). The CF component was ~50% larger in power than both HF and also LF (when present). Spectral analysis at increasing count levels (i.e., with only the events with a weight \geq the considered level) indicated that all rhythms were carried by burst activity and its modulations. A modulation index of HF over CF, $MI_{HF/CF}$ was extracted from dynamic (i.e., ventilation cycle by ventilation cycle) folded histograms of counts. $MI_{HF/CF}$ was significantly higher in the group without LF (0.65 ± 0.20 , mean \pm SD, $n=4$) than in that with LF (0.41 ± 0.07 , $n=9$). Burst activity can be a key element in the interactions between cardiovascular variability rhythms.

Keywords - Sympathetic outflow, burst activity, beat-to-beat variability, cardiac rhythm.

I. INTRODUCTION

Rhythms synchronous to cardiovascular variability and autonomic control oscillations have been described at various levels of the central nervous system and autonomic nervous system; i.e., the Mayer's low frequency (LF) waves and the respiratory high frequency (HF) ones [1, 2, 3]. Nonetheless, they are accompanied by faster rhythms that can not be put in relation with cardiovascular variability by means of classical methods in time and frequency domain, simply because they are found at a frequency equal or higher than the cardiac frequency (CF) itself [1].

Complex interactions between rhythms have been observed both in the cardiovascular variability signals [4] and in neural activity [5] and it is well known that non linear mechanisms do not permit to separate frequency bands but on the contrary are capable to transpose the spectral contents.

Multifiber recordings hardly permit to analyze the dynamics of single action potentials (spikes), but do offer a rich information about synchronization patterns of different fibers and their coupling to other processes such as heart contraction and ventilation.

Little is known about the processing of multifiber activity, beyond the classical methods of mediating over specific time ranges (e.g., one cardiac cycle) [5] or low pass filtering. Therefore, it is developed a novel algorithm that recognizes burst activity and represents it as a series of events weighted by the estimated number of synchronous spikes. Subsequent spectral and synchronization analyses are carried out at different weight levels considering only bursts representing a number of spikes equal or above the specified level.

II. METHODOLOGY

13 cats were decerebrated under anesthesia with an intercollicular section, vagotomized and artificially ventilated by a Harvard pump at 18 cycle/min monitoring the pCO_2 and pO_2 levels. Recordings were carried out after cerebral death and after the anesthesia effect was exhausted. Preganglionic sympathetic outflow to the heart was recorded from few isolated fibers of the 3rd white ramus by means of platinum electrodes. After amplification and antialiasing filtering, the neural signal was directly recorded and next sampled at 3 kHz sampling rate. Contemporaneously the ECG tracing, ventilation pump flow and arterial pressure were also recorded and sampled at 300 Hz. Recordings in control (i.e., decerebrate) condition lasted about 5 min; other conditions with activation maneuvers and denervations were also

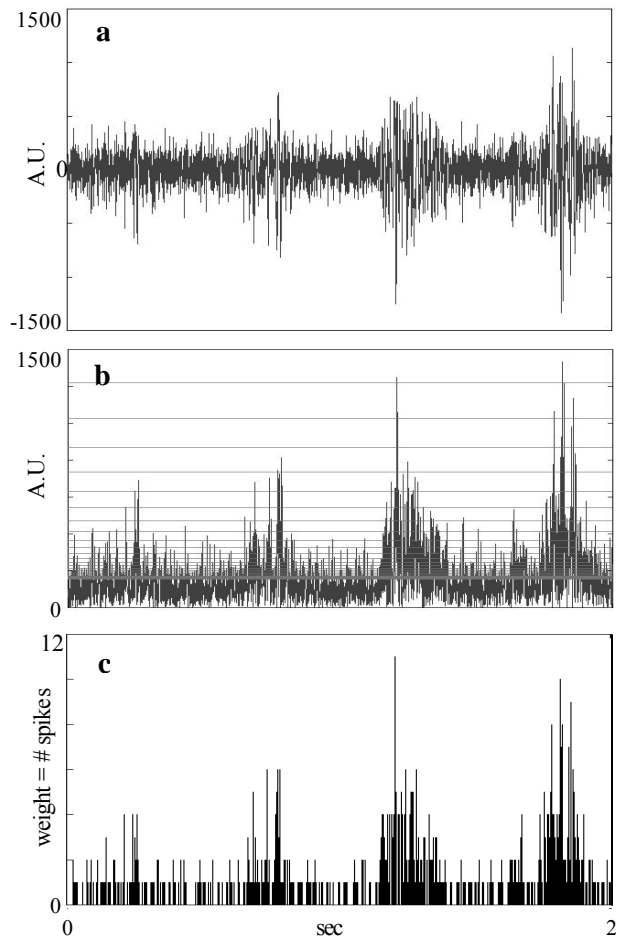


Fig. 1. Neurographic multifiber signal (a). Rectified signal superimposed to multiple thresholds (b). Weighted event series: bar height indicates the estimated number of synchronous spikes (c).

Report Documentation Page

Report Date 25 Oct 2001	Report Type N/A	Dates Covered (from... to) -
Title and Subtitle Burst Activity and Heart Rhythm Modulation in The Sympathetic Outflow to the Heart	Contract Number	
	Grant Number	
	Program Element Number	
Author(s)	Project Number	
	Task Number	
	Work Unit Number	
Performing Organization Name(s) and Address(es) Department of Biomedical Engineering Polytechnic University of Milan Milan Italy	Performing Organization Report Number	
Sponsoring/Monitoring Agency Name(s) and Address(es) US Army Research, Development & Standardization Group (UK) PSC 802 Box 15 FPO AE 09499-1500	Sponsor/Monitor's Acronym(s)	
	Sponsor/Monitor's Report Number(s)	
Distribution/Availability Statement Approved for public release, distribution unlimited		
Supplementary Notes Papers from 23rd Annual International Conference of the IEEE Engineering in Medicine and Biology Society, October 25-28, 2001, held in Istanbul, Turkey. See also ADM001351 for entire conference on cd-rom.		
Abstract		
Subject Terms		
Report Classification unclassified	Classification of this page unclassified	
Classification of Abstract unclassified	Limitation of Abstract UU	
Number of Pages 3		

recorded but are not considered here. Sampled signals were stored on a PC for further processing.

Multifiber activity was analyzed by a specifically designed program in order to extract event series in which each event was weighted by the subtended area of the rectified signal taken as the estimated number of firing fibers. As shown in Fig.1a, the single spikes are hardly recognizable in the neural tracing due to superpositions and noise but bursts of activity are clearly detectable.

The mean value is first subtracted and the resulting signal is rectified. Fig.1b shows how the rectified signal is compared with multiple thresholds positioned at levels increased by a geometric progression. Multiple thresholds are used to decide whether a multiple event can be split into two subsequent events of less weight. The procedure is activated when the signal is above the first threshold and works as follows: 1) the points in which whatever threshold is passed (no matter whether downward or upward) are detected; 2) the area subtended by the rectified signal between two subsequent threshold passages is computed; 3) an event is positioned at the center of this time interval if and only if the unitary area estimated for a single spike is exceeded; 4) the truncated value of the ratio between the area in the interval and the unitary area is the weight of the event. Fig.1c displays the detected events by means of bars indicating the event times by their position and the event weights by their heights.

It can be noted that to detect an event of unitary weight it is not sufficient to exceed the first threshold but also a sufficient area must be subtended when the signal is above threshold. In addition when a steep rise or fall is present and two subsequent thresholds are passed in a short time, no event is detected due to insufficient subtended area. These characteristics render the algorithm robust in respect to noise and to burst shape features and represent the main rationale for a multiple threshold strategy.

The weighted event series is also named counted signal; in fact, if a pulse (Dirac's distribution) multiplied by the weight is positioned in correspondence to each event, a signal is obtained which carries the information about the instantaneous firing rate exactly as if clusters of unitary events were considered. Grouping the single events into multiple events permits to fix a threshold to the weight of events to be considered and separate burst activity from sparse activity. In the following a "counted signal of level n " will indicate that only events with a weight $\geq n$ are considered while smaller ones are discarded. All processing procedures were applied to all possible levels from level 1 (i.e., the counted signal with all events) up to the maximum detected weight (usually 15).

The spectrum of counts was obtained by a smoothed periodogram algorithm. For a frequency analysis up to 5 Hz, 35 sec long frames (66% overlap) were windowed (Hann's window), FFT transformed and averaged over the entire 5 min recording. The same procedure was applied for the various count levels. As shown in Fig.2 the spectra of counts display the low frequency (LF around 0.1 Hz) and high frequency (HF = 0.33; i.e., the ventilation frequency in this experimental condition) that can be detected also in beat by beat variabilities but also a main spectral peak at cardiac frequency (CF) that can be analyzed only by processing

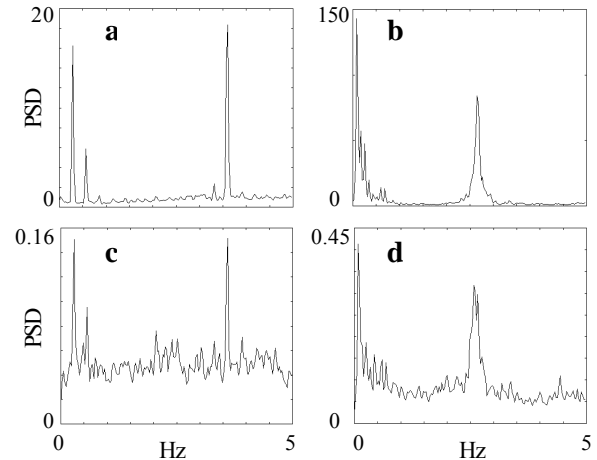


Fig. 2. Power Spectral Densities [(spikes/sec)²/Hz] of all events (level 1, see text) in a case without (a) and with (b) LF. Same spectra computed at level 7 (c and d, respectively).

directly the neural activity by this or similar methods. The P_{LF} , P_{HF} , P_{CF} power is evaluated by considering three bands of 0.01-0.13 Hz, 0.13-0.53 Hz, and mean $CF \pm 0.2$ Hz, respectively. Both absolute and percent powers were tabulated.

Synchronization to the ventilation cycle on a period of $1/HF=3.33$ sec was evaluated by means of a folded histogram of counts as shown in Fig.3a. The histogram is obtained simply by folding the counted signal in correspondence to each maximum of the ventilation signal and summing up the weights of events present at the various phases of the ventilation cycle subdivided into bins of 33.3 msec. This histogram gives an average and static view of how the neural discharge is influenced by the ventilation phase. In order to analyze how faster rhythms (mainly CF rhythm) are modulated by ventilation and if they can be phase locked to it, a dynamic folded histogram was also considered, in which the counted signal was displayed ventilation period by ventilation period, as in Fig.3b. This plot is much like a raster scan of counts triggered by ventilation but a smoothing is obtained by grouping the events into the 33.3 msec long bins.

In the dynamic folded histogram the activity synchronous with heart period is clearly seen and also it can be appreciated that the different response to ventilation phase is mainly obtained by means of a modulation of the burst activity synchronous to the heart beat. Therefore, a modulation index of HF over CF, $MI_{HF/CF}$, is obtained with the following steps: 1) the value of the highest and the lowest cardiac burst (HCB and LCB respectively) is detected in each ventilation cycle; 2) highest and lowest bursts are averaged over all ventilation cycles thus obtaining HCB_{AV} and LCB_{AV} ; 3) finally,

$$MI_{HF/CF} = (HCB_{AV} - LCB_{AV}) / LCB_{AV} \quad (1)$$

III. RESULTS

The average firing rate detected was 223 ± 64 (mean \pm SD) spikes/sec. The activity was unequally subdivided into events of different levels: e.g., events with a weight of 1 were

149±46 /sec, those with weight 5 were 3±0.6/sec and with weight 7 were 0.5±0.23/sec.

Spectral analysis of counts revealed that the CF was always the main rhythm in sympathetic discharge. A clear HF peak was always present; on the contrary various levels of LF were found and in 4 out of the 13 cats this activity was virtually absent. Therefore, it was decided to separate the group into a subgroup with LF (SG_{LF} , $n=9$) and into a subgroup without LF ($SG_{LF,NOT}$, $n=4$).

In SG_{LF} , $P_{LF}\%=20.91\pm15.58$, $P_{HF}\%=19.72\pm5.9$, $P_{CF}\%=26.2\pm8.49$; while in $SG_{LF,NOT}$, $P_{LF}\%=1.3\pm0.56$, $P_{HF}\%=22.23\pm13.12$, $P_{CF}\%=33.08\pm17.13$.

Interestingly, the spectral peaks are recognizable also in a spectral analysis performed at level 7, as shown in Fig.2c,d. Indeed, spectral peaks were detected even at higher levels, thus indicating that burst activity, rather than sparse activity, carries the LF, HF and CF rhythms. Only at levels above 12 spectra of counts became flat indicating that highest level events occur randomly.

The folded histogram always revealed the effect of ventilation on neural discharge. In Fig.2 the histogram relevant to all events (level 1) is shown in black, while that relevant to level 3 (i.e., all events of lower weight are cut off) is represented by the white bars. It can be appreciated that also events of higher weight are modulated by ventilation (this is true also for level up to 12, but it is not shown due to the low scale of the relevant histograms).

More interestingly, with the dynamic folded histogram it was possible to detect the presence of intermittent synchronization patterns between the CF and the HF. In the example of Fig.3b, it can be appreciated a stationary phase relationship in the ventilation cycles from 1 to 15 and from 52 to 60. In these epochs exactly 8 cardiac cycles fit into a ventilation cycle. In the intermediate epoch (ventilation cycles from 16 to 51) a regular phase shift is on the contrary present indicating quasiperiodicity.

Moreover, the ratio between the HF and the CF spectral components did not display significant changes between SG_{LF} and $SG_{LF,NOT}$ (0.84 ± 0.43 and 0.90 ± 0.70 respectively); while, on the contrary, the $MI_{HF/CF}$ obtained from the dynamic histogram was significantly higher in the latter group (0.41 ± 0.07 and 0.65 ± 0.20 , respectively). This indicates that, in absence of LF oscillations, ventilation has a higher modulation on the burst synchronous to the heart and also this effect is mainly non-linear and, therefore, is not detected by spectral analysis.

V. CONCLUSION

The proposed algorithm of burst activity detection and weighing extends the band of observed rhythms and also permits to evaluate its contribution in forming slower variability rhythms.

Spectral analysis carried out over higher burst levels indicates that LF and HF variability oscillations are conveyed by burst activity, which in addition appears to be synchronous to the heart beat at the CF. The HF ventilation rhythm appears as a modulation of the CF bursts and the relevant modulation index is blunted by LF oscillations.

These preliminary results can introduce to a novel methodology for the analysis of rhythm interactions in

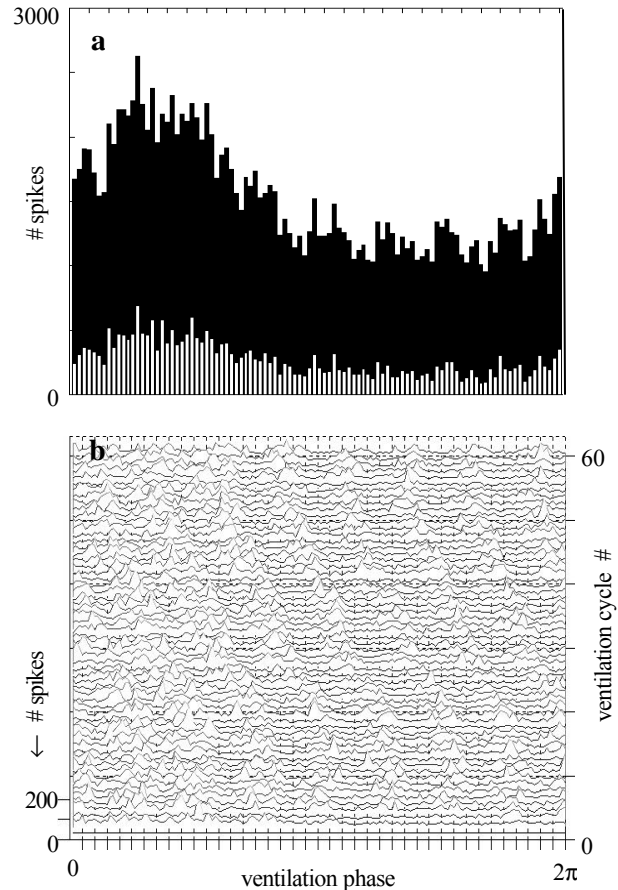


Fig. 3. Cumulative folded histogram of spikes in the ventilation cycle at level 1 (a, black) and at level 3 (a, white). Dynamic (ventilation cycle by ventilation cycle) folded histogram (b)

multiunit neurographic recordings.

REFERENCES

- [1] S.M. Barman and G.L. Gebber, "Rapid rhythmic discharges of sympathetic nerves: sources, mechanisms of generation, and physiological relevance," *J. Biol. Rhythms*, vol.15, pp. 365-379, 2000.
- [2] R. Vandenhousten, M. Lambertz, P. Langhorst, R. Grebe, "Nonstationary time-series analysis applied to investigation of brainstem system dynamics," *IEEE Trans. Biomed. Eng.*, vol. 47, pp. 729-737, 2000.
- [3] M. Massimini, A. Porta, M. Mariotti, A. Malliani, N. Montano, "Heart rate variability is encoded in the spontaneous discharge of thalamic somatosensory neurones in cat," *J. Physiol.*, vol. 15;526 Pt 2, pp. 387-396, 2000.
- [4] A. Porta, S. Guzzetti, N. Montano, M. Pagani, V. Somers, A. Malliani, G. Baselli, S. Cerutti, "Information domain analysis of cardiovascular variability signals: evaluation of regularity, synchronisation and co-ordination," *Med. Biol. Eng. Comput.*, vol. 38, pp. 180-188, 2000.
- [5] A. Porta, G. Baselli, N. Montano, T. Gnechchi-Ruscione, F. Lombardi, A. Malliani, S. Cerutti, "Classification of coupling patterns among spontaneous rhythms and ventilation in the sympathetic discharge of decerebrate cats," *Biol. Cybern.*, vol. 75, pp. 163-72, 1996.